International Journal of Applied Pharmaceutics

ISSN- 0975-7058 Vol 16, Issue 6, 2024

Original Article

DESIGN, OPTIMIZATION AND EVALUATION OF RANOLAZINE FAST-DISSOLVING FILMS EMPLOYING MANGO KERNEL STARCH AS A NEW NATURAL SUPERDISINTEGRANT

MEDISETTY GAYATRI DEVI, SANTOSH KUMAR R.*

Department of Pharmaceutics, GITAM School of Pharmacy, Visakhapatnam, Andhra Pradesh-530045, India
***Corresponding author: Santosh Kumar R.; *Email: srada@gitam.edu**

Received: 19 May 2024, Revised and Accepted: 17 Sep 2024

ABSTRACT

Objective: The BCS class II cardiovascular medication, Ranolazine (RZN), is characterized by limited solubility and inadequate oral absorption. The objective of the current research is to develop a natural superdisintegrant in the formulation of Fast-Dissolving Films (FDFs) of Cardio Vascular Drug (CVD) RZN to enhance its dissolution rate, solubility, absorption, and therapeutic action.

Methods: Mango Kernel Starch (MKS) is isolated by grinding the kernels, forming a slurry with water, filtering, and using repeated centrifugation and washing to purify the starch, which is then dried. The obtained starch is collected. Along with obtained natural superdisintegrant MKS, Maltodextrin (MDX) and Sodium Starch Glycolate (SSG) were also utilized in the fabrication of FDFs containing RZN via the solvent casting technique. A total of eight formulations (RF1 to RF8) were developed employing a 2^3 factorial design, using the natural superdisintegrant alone at a concentration of 5% and in combination with other superdisintegrants.

Results: The prepared MKS was found to be free-flowing, fine, amorphous, insoluble in organic solvents, and exhibiting 0.17% solubility in water with a swelling index of 89.95%, indicating superdisintegrant properties. Fourier-transform infrared spectroscopy (FTIR) studies and Differential scanning calorimetry (DSC) analysis indicated that there was no drug-excipient interaction. The films prepared with a 5% concentration of the MKS showed good physical properties and resulted in an increased drug dissolution rate, with 99.78 % of the drug dissolved within 10 min, along with the lowest disintegration time of 13.45 sec.

Conclusion: The research successfully isolated a new superdisintegrant, MKS and formulated FDFs of the poorly water-soluble drug RZN. The MKS was found to be an effective superdisintegrant with no drug interactions, producing films with good physical and mechanical properties, increasing the drug dissolution rate, and providing rapid disintegration with improved relative bioavailability.

Keywords: Fast dissolving films, FDFs, Ranolazine, Solvent casting technique, Super disintegrant, Mango kernel starch

DOI: https://dx.doi.org/10.22159/ijap.2024v16i6.51506 Journal homepage: https://innovareacademics.in/journals/index.php/ijap

INTRODUCTION

The oral route is the most often used since it is the easiest to administer and results in high patient compliance. Oral solid dose forms account for over 60% of all dosage forms; tablets and capsules are the most often used types [1]. However, there are several limitations for geriatric, paediatric, or dysphagia patients, people with difficulty swallowing, and even in animals [2]. As an alternative method to overcome these limitations, orally disintegrating systems were developed, aiming for a fast release of the drug without water ingestion, also enabling drug absorption directly through oral mucosa to enter systemic circulation, avoiding first-pass hepatic metabolism [3].

Fast-dissolving films (FDFs) are one such novel approach to increase consumer acceptance by rapid dissolution and self-administration without water or chewing. The need for non-invasive delivery systems continues due to patients' poor acceptance and compliance with existing delivery regimes, the limited market size for drug companies and drug uses, coupled with high cost of disease management [4]. Usually, the casting technique is used to prepare FDFs with natural polymers, and other techniques like hot-melt extrusion [5] are frequently used to process synthetic polymers. FDFs can also be prepared by utilizing other techniques such as electrospinning [6], freeze-drying [7], and heat-drying methods [8], which may affect certain characteristics, particularly film thickness.

The choice of the optimal usage of superdisintegrants remains difficult since they must be able to dissolve in the oral cavity as quickly as feasible and cost-effectively. Much research has been carried out on natural superdisintegrants like Starch derivatives (Corn and potato starch), Alginates, Guar gum, Chitosan and Plantago ovata [9].

Existing research focuses on the efficacy of natural starch as a superdisintegrant and positions Mango Kernel Starch (MKS) as a superior alternative [10]. MKS is increasingly utilized as a superdisintegrant in the optimization and design of FDFs due to its exceptional disintegration efficiency, biocompatibility, and cost-effectiveness. Its ability to rapidly absorb water and swell ensures quick breakdown upon contact with saliva, a critical feature for FDFs. As a natural, non-toxic material, MKS reduces the risk of adverse reactions, making it suitable for pharmaceutical applications. Additionally, its use promotes sustainability by valorizing a by-product of mango processing, aligning with eco-friendly manufacturing practices. Accordingly, we examined the literature in this work to optimize and design FDFs of Ranolazine (RZN) using MKS as a natural superdisintegrant [11].

The novelty of this research lies in the introduction of MKS as a novel superdisintegrant in the formulation of FDFs for the antihypertensive drug RZN. Addressing the challenge of poor water solubility and limited bioavailability, this study explores the potential of MKS to enhance the disintegration time and drug dissolution rate. Traditional superdisintegrants such as Maltodextrin (MDX) and Sodium Starch Glycolate (SSG) have been widely used, but the integration of MKS presents a promising alternative due to its natural origin and superior performance [12].

Statistical analysis using 2^3 factorial design is a method employed for optimizing the formulation of superdisintegrants in the manufacturing of films [13]. This approach allows researchers to systematically evaluate the three critical factors, each at two levels. This study aims to enhance the dissolution rate with rapid disintegration and increased relative bioavailability. Such precision in formulation has the potential to improve therapeutic efficacy and patient compliance, contributing significantly to advancements in pharmaceutical research [14].

MATERIALS AND METHODS

Materials RZN, the active pharmaceutical ingredient (API), was a gift sample obtained from Hyderabad-based Hetero Pvt Ltd. HPMC E15

was purchased from TM Media Delhi, MKS was extracted in the laboratory setting. SSG and Propylene Glycol (PG) were purchased from SD Fine Chemicals Ltd. in Mumbai. MDX and citric acid were purchased from Gattefosse India Private Limited in Mumbai, and mannitol was purchased from Loba Chemie Pvt Ltd in Maharashtra. These components, sourced from reputable manufacturers and suppliers, were integral to the development of the formulation.

MKS preparation and characterization

MKS extraction

The starch from the mango kernels is extracted by using the following process. The mango kernels were blended with a solution containing 0.16% sodium metabisulphate. The resulting mixture was passed through a 100 sieve mesh, followed by a 300 sieve mesh; after allowing the mixture to settle, the supernatant was carefully poured off, and distilled water was added to the remaining residue. The dispersion was then subjected to centrifugation for 5 min at 5000 RPM. The upper layer, which did not contain starch, was removed mechanically, and the obtained residue was washed with distilled water. This process of washing and centrifugation was continued multiple times till the starch was completely free from any other residue except starch. Finally, the obtained starch was dried at a temperature of 45 °C for 24 h and subsequently pulverized [15].

Characterization of MKS

Starch yield

The % yield of isolated starch was determined by using the below equation [16]

$$\text{Starch Yield (\%)} = \frac{\text{Initial weight - Final weight}}{\text{Initial weight}} \text{X100}$$

Starch test

The extracted sample is mixed with the Lugol's solution (a solution of potassium iodide with iodine in water). It then turns out into a bright blue-black colour that indicates the presence of starch. The solution's colour doesn't change if there is no starch present [17].

Solubility

The extracted MKS was weighed at 100 mg and placed into eight separate test tubes. In each test tube holding the sample, 10 ml of different solvents like ethanol, propylene glycol, acetone, chloroform, hydrochloric acid, liquid paraffin, n-hexane, and water was added in turn. The test tubes were shaken, the solubility and dispersibility were noted, and the findings were recorded [18].

pH

Using a digital pH meter, the pH of 1.0% w/v suspensions of mango starch was measured in triplicate, and the findings were noted [19].

Swelling index

MKS 200 mg was added to two test tubes (graduated), having 10 ml of liquid paraffin and distilled water, and mixed. The two test tubes having MKS dispersion were kept aside for 12 h. After the duration of 12 h, the volume of sediment was noted. The swelling index is calculated by the given below equation [20].

$$\text{S.I (\%)} = \frac{\text{Volume of sediment- Volume of sediment in light liquid paraffin}}{\text{Volume of sediment in light liquid paraffin}} \text{ X 100}$$

Melting point

The melting point of the MKS was determined by Differential scanning calorimetry (DSC) [21].

Moisture absorption

The hygroscopic nature of MKS was assessed at room temperature and 84% relative humidity in a closed desiccator [22].

Drug excipient compatibility

Fourier-transform infrared spectroscopy (FTIR)

300 mg of previously dried potassium bromide was taken and finely ground; the crystals were turned into a powder, Then, 2 g of MKS was added and thoroughly triturated. The infrared spectrum was produced using a potassium bromide (KBr) disc and scanning from 400 to 4000 cm^{-1}.

DSC

Samples consisting of 15 mg of starch and 5 mg of distilled water were prepared on closed aluminum pans. Before the measurements, the samples were allowed to stand for the entire night. The heating function of a PerkinElmer 8500 universal calorimeter, operating between 28 °C and 250 °C, was employed to analyze peak temperature using a technique called DSC.

Formulation development of FDFs

RZN FDFs preparation using 2^3 factorial designs

To optimize the formulation variables 2^3 factorial design was used, focusing on the concentrations of MKS, MDX, and SSG as the main factors. These choices were based on preliminary studies conducted before setting up the experimental design. Following this plan, we prepared multiple batches of RZN according to the factorial design, resulting in a total of 8 runs generated using the Design Expert® software. The present investigation examined two key response variables: disintegration time and PD_{10}-the percentage of drug dissolved within a 10 min timeframe. Analysis of the experimental results was performed using ANOVA, fitting the response variables within the framework of the factorial design. Detailed information on the investigated response variables and the design matrix can be found in table 1 [23].

Table 1: Optimization variables and their levels used in RZN FDFs factorial design

Variables	Low (-1)	High (+1)
MKS (%)-A	0	5
MDX(%)-B	0	5
SSG (%)-C	0	5

Preparation of RZN FDFs

The formulation process began by dispersing 350 mg of HPMC E15 and superdisintegrants in sufficient quantity (70%) of distilled water, which was then stirred for 2 h at 2000 RPM on a magnetic stirrer at room temperature (Solution A). Separately, a mixture containing 350 mg of RZN and 50 mg of citric acid was dispersed in an adequate quantity of distilled water (30%) containing 150 mg of plasticizer (PG) and stirred for 1 h (Solution B). Solution B and 50 mg of mannitol were slowly added to solution A while manually agitating to ensure uniform distribution. After achieving a clear solution, it was left undisturbed for 6 h to release any remaining bubbles or air. Subsequently, the solution was decanted onto a petri dish and dried using a hot air oven at 40 °C for 24 h. The resulting films were then cut into 2x2 cm^2 pieces and stored in aluminium sachets within a desiccator [24].

Evaluation of prepared RZNFDFs

Morphological studies

The three individual 2x2 cm^2 FDFs of each formulation were visually inspected for homogeneity, transparency, colour, and surface quality [25].

Weight variation studies

The weight of three 2x2 cm^2 FDFs of each formulation was noted by using an electronic weighing balance [26].

Thickness

The thickness of three samples, each measuring 2x2 cm^2, from every formulation was measured with a screw gauge with a 0-10 mm range and a least count of 0.01 mm. The collected data was analysed to calculate the mean and standard deviation [27].

***In vitro* disintegration time**

A Petri dish with 25 ml of 6.8 pH buffer solution was placed on a thermostat shaker set to 50 RPM and at 37±0.3 °C; the temperature was maintained. The 2x2 cm^2 size of the film was placed in a petri dish, and the time taken for the film to disintegrate was then recorded [28].

Surface pH

The 2x2 cm^2 film was first placed in a petri dish and wetted with distilled water. Subsequently, it was brought into contact with the electrode of a pH meter, and the pH was noted [29].

Drug content uniformity

The 2x2 cm^2 film was sliced and placed into a 100-millilitrevolumetric flask with phosphate buffer, and it was agitated using a mechanical shaker to achieve uniformity. After filtration, the drug content was subsequently measured spectroscopically at 296 nm [30].

$$\text{Drug content (\%)} = \frac{\text{Actual amount of drug}}{\text{Theoretical amount of drug}} \text{ X } 100$$

Tensile strength

The FDFs tensile strength was measured by calculating the thickness, width, and load force at failure (the load at which the film breaks). The load force at failure was obtained using a 50 kg weighted cell and an Instron testing device. Film of 2x2 cm^2 size was positioned vertically in between the two clamps. At a rate of 100 mm per minute, the upper clamp was pulled while keeping the lower clamp stationary. The weight at which the film broke was noted. The obtained values were then used in the formula below to calculate the tensile strength [31].

$$\text{TS(\%)} = \frac{\text{Load force at failure}}{\text{Film Thickness}} \text{ X Film width}$$

Percentage elongation (%E)

The % elongation of the film was measured by the initial length of the FDFs and the increased length of the FDFs. The increased length of the film was measured by using a 50 kg weighted cell and an Instron testing device. Each sample (2x2 cm^2) was securely held in a vertical position between two clamps. The films were then subjected to tension at a rate of 100 mm per minute by the top clamp, while the bottom clamp remained fixed. The obtained initial length of the film and length of the film after fracture were used in the below formula to calculate the percentage elongation of the film [32].

$$\text{Percentage Elongation} = \frac{\text{Increased length of film}}{\text{Initial length of film}} \text{X } 100$$

Folding endurance

The FDFs folding endurance was measured by the number of times the film was folded at the same location until it broke or reached the folding limit [33].

Percent moisture absorption (uptake) and moisture loss

Initially, the weight of the 2x2 cm^2 film was noted, and the films were subjected to 75% relative humidity at room temperature for a week. Then the final weight of the film was noted. The percentage moisture absorption is calculated by using the below formula [34].

$$\text{Percentage moisture absorption} = \frac{\text{Final weight of film - Initial weight of film}}{\text{Initial weight of film}}$$

Desiccators containing anhydrous calcium chloride were used to ensure the films maintained their weight. The films were removed and weighed after 3 d. The formula for determining moisture loss and moisture absorption rates is as follows.

$$\text{Percentage moisture loss} = \frac{\text{Initial weight of film - Final weight of film}}{\text{Initial weight of film}} \text{ X } 100$$

***In vitro* dissolution studies**

In vitro dissolution studies were performed by using a modified type 5 dissolution apparatus. Each film, sized at 2x2 cm^2 containing 40 mg of RZN, was placed on a watch glass and covered with wire mesh made of nylon. The assembly was then placed into a dissolution flask containing 500 ml of artificial saliva (phosphate buffer of pH 6.8) as the dissolution medium. The rotation speed was limited to 50 RPM, and the temperature was maintained at 37 °C. At specified intervals of 5, 10, 15, 20, 25, 30, 45, and 60 min, a 5 ml sample was withdrawn. After each withdrawal, an equal volume of fresh dissolution medium was added. Appropriate dilutions were performed on the dissolution medium, and the samples were analysed at 272 nm. The measurements were carried out three times [35].

***In vivo* study design**

The study was carried out as a crossover randomized block design in male Wistar rats, employing the pure drug (RZN) and optimized FDFs of RZN (RF2) formulated by using MKS as a novel superdisintegrant [36].

Animal care facilities

Wistar rats were kept together in a house by providing free access to water and food in a clean room, maintaining the temperature at 20-25 °C. For 12 h the animals are kept in a light-dark cycle each day.

The experimental procedure is explained in the following fig. 1

The analytical method followed to study the blood samples in rat plasma

The validated HPLC method was used for the study. Method conditions are depicted in the following table 2 [37].

Pharmacokinetic studies

The study examined several pharmacokinetic parameters, including the C_{max} (maximum plasma concentration), t_{max} (the time at which maximum plasma concentration occurred) area under the plasma concentration-time curve (AUC), Bioavailability (BA), absorption rate constant (Ka) and elimination rate constant (Ke).

Table 2: HPLC method condition for RZN

Parameters	Method conditions
Equipment used	HPLC equipped with Shimadzu LC Solutions
Column	Shim-pack C18 column, Internal diameter: 4.6 mm, Length: 150 mm, Pore size: 120 Å.
Mobile Phase	10 mmol ammonium acetate and Methanol (24:76 %v/v)
loop injector	Shimadzu 7D Rheodyne
Injector type	Binary pumping mode
Run time	10 min
Flowrate	1.0 ml/min
Detector	Photo Diode Array (PDA)
Injector Volume	20 µl**

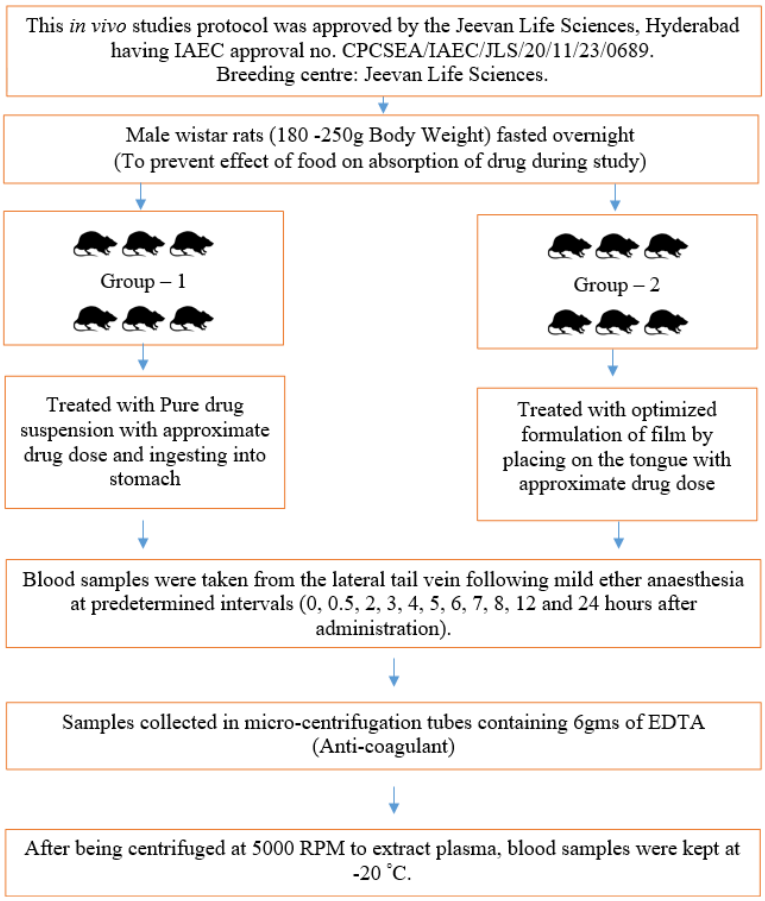

Fig. 1: Experimentation on male wistar rats

RESULTS AND DISCUSSION

Characterization of MKS

The prepared MKS was found to be free-flowing, fine, and amorphous. The physical properties of the MKS are summarized in table 3. MKS is insoluble in organic solvents and slightly soluble in water up to 0.17 %. The pH was measured at 4.0, and the melting point is 89.43 °C, which is suitable for the formulation of FDFs. The swelling index was found to be 89.95%, indicating that MKS has superdisintegrant properties.

Table 3: Physical properties of MKS

Content	Observation
Solubility	Insoluble in organic solvents, Aqueous solubility is 0.17%
pH (1% w/v aqueous dispersion)	4.0±0.42
Yield (%)	64.56± 1.2%
Melting Point (°C)	89.43 °C
Swelling Index %	89.95±1.2%
Moisture absorption	2.0±0.2 %
Viscosity 1% (cps)	1.07 cps

Data are expressed as mean±SD, n=3

FTIR studies of MKS

The MKS FTIR spectrum was analysed, revealing a peak at 3417.98 cm^{-1} due to hydrogen bonding in the starch molecule. Other characteristic peaks associated with functional groups present in its molecular structure like the C-H stretch are observed between 2800-3000 cm^{-1}, with a specific wavenumber of 2933.83 cm^{-1}. The C-O (alkoxy) band falls within 1000-1200 cm^{-1}, with a wavenumber of 1109.11 cm^{-1}. Lastly, the C-O-C stretch is found in the range of 900-1100 cm^{-1}, with a wavenumber of 1043.52 cm^{-1}.

MKS DSC

MKS showed Tp – peak temperature and Tc-conclusion temperature ranged from 89.43 °C-129.42 °C.

Drug excipient compatibility studies

The RZN pure drug FTIR spectrum characteristic bands are observed at functional groups like Pure RZN characteristic bands at 3430.51 cm^{-1}(N-H), 2923.22 cm^{-1} (O-H), 1479.45 cm^{-1}(C-C) 2359.38 cm^{-1}(C-H), showed by RZN FTIR spectrum, whereas characteristic bands 3447.87 cm^{-1}(N-H), 2926.11 cm^{-1}(O-H), 1460.16 cm^{-1}(C-C), 2359.98 cm^{-1}(C-H) peaks were observed in MKS FTIR spectrum. The hydroxyl groups in both RZN and MKS can engage in hydrogen bonding interactions. It was concluded that MKS did not interact with the drug. The thermogram of the RZN along with the MKS exhibited a sharp endothermic peak at 119.85 °C, which corresponds to a pure RZN melting point of 120-124 °C that indicates the prepared MKS is compatible with the RZN.

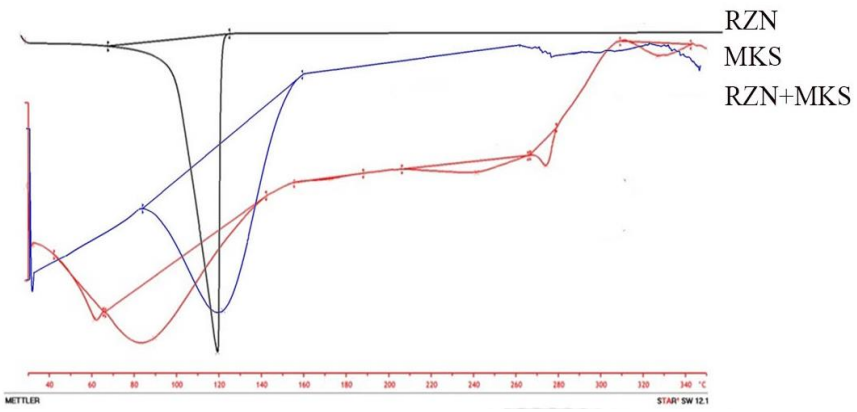

Fig. 2: DSC thermogram of pure MKS, RZN and their combinations MKS+RZN

Optimization of the independent variables

Based upon the preliminary studies, the films prepared with a 5 % concentration of the superdisintegrants, 50 to 60 % of the film-forming polymer, and 15% of the plasticizer were non-sticky, uniform, and clear. It was observed that the formulation with a 5% natural superdisintegrant showed an increase in dissolution time (DT) and a decrease in disintegration time.

Effect of formulation factors on dependent variables *in vitro* disintegration time and Percentage drug dissolved in 10 min

In vitro Disintegration Time =-71.00+51.75A+44.00B+49.00C-49.75AB-52.25AC-51.50 BC+48.75ABC

Percentage dissolved in 10 min =+79.29+10.71A+4.09B+8.67C-13.29AB-13.50AC-12.75 BC-8.07ABC

An inference can be drawn by evaluating the statistical significance (positive or negative) and the magnitude of the variable in a polynomial equation. By seeing the above two polynomial equations, it can be interpreted that the factor ABC, A, B and C has a positive effect on the DT, while AB, AC, and BC have a negative effect on the DT.

The A, B, and C factors had a positive effect on the PD_{10} and AB, AC, BC and ABC have a negative effect on the PD_{10}.

It is necessary to know the individual and combination effects of the superdisintegrants which were used for the formulation of RZNFDFs by ANOVA. ANOVA of *in vitro* disintegration time (table 4) and ANOVA percentage of drug dissolved in 10 min (table 5) results indicate that the individual and combination effects of the MKS, MDX and SSG were significant (P<0.05).

Table 4: Disintegration time ANOVA for RZN FDFs

Source of variation	df	Sum of squares	mean square	F-value	Result
Replicates	2	1.878	0.939	2.126	P>0.05
Treatments	7	413976.000	59139.429	133918.641	P<0.05
A-MKS	1	64273.500	64273.500	145544.521	P<0.05
B-MDX	1	46464.000	46464.000	105215.689	P<0.05
C-SSG	1	59401.500	59401.500	134512.091	P<0.05
AB	1	57624.000	57624.000	130487.020	P<0.05
AC	1	65521.500	65521.500	148370.562	P<0.05
BC	1	63654.000	63654.000	144141.690	P<0.05
ABC	1	57037.500	57037.500	129158.916	P<0.05
Pure Error	14	6.183	0.442		
Cor Total	23	413976.000			

ANOVA-Analysis of variance, Degrees of freedom-df, Sum of square-S. S, Non-significant-P>0.05, Significance-P<0.05

Table 5: Percentage dissolved in 10 min ANOVA for RZN FDFs

Source of variation	df	Sum of squares	mean square	F-value	Result
Replicates	2	1.878	0.939	2.126	P>0.05
Treatments	7	413976.000	59139.429	133918.641	P<0.05
A-MKS	1	64273.500	64273.500	145544.521	P<0.05
B-MDX	1	46464.000	46464.000	105215.689	P<0.05
C-SSG	1	59401.500	59401.500	134512.091	P<0.05
AB	1	57624.000	57624.000	130487.020	P<0.05
AC	1	65521.500	65521.500	148370.562	P<0.05
BC	1	63654.000	63654.000	144141.690	P<0.05
ABC	1	57037.500	57037.500	129158.916	P<0.05
Pure Error	14	6.183	0.442		
Cor Total	23	413976.000			

ANOVA-Analysis of variance, Degrees of freedom-df, Sum of the square-S. S, Non-significant-P>0.05, Significance-P<0.05

The 3D surface response plot and contour plot in fig. 4 and 5 show the different independent variables' effect on the percentage of drug dissolved in 10 min and *in vitro* disintegration time. The RZN FDFs *in vitro* disintegration time was found to be greater with MKS (A) concentration at a range of 4-5% and MDX (B) concentration at a range of up to 1 %. The RZN FDFs *in vitro* disintegration time was found to be

greater with MKS (A) concentration in the range of 4-5 % and SSG (C) concentration at a range of up to 2 %. The RZN FDFs *in vitro* disintegration time was found to be greater with MDX (B) concentration at a range of up to 1 % and SSG (C) concentration at a range of 2-5 %.

The percentage of drug dissolved in 10 min of RZN FDFs was found to be greater with MKS (A) concentration in the range of 4-5% and MDX (B) concentration at a range of 4-5 %. The percentage of drug dissolved in 10 min of RZN FDFs was found to be greater with MKS (A) concentration at a range of 4-5% and SSG (C) concentration at a range of up to 4-5%. The percentage of drug dissolved in 10 min of RZN FDFs was found to be greater with MDX (B) concentration at a range of up to 4-5 % and SSG (C) concentration at a range of 4-5%.

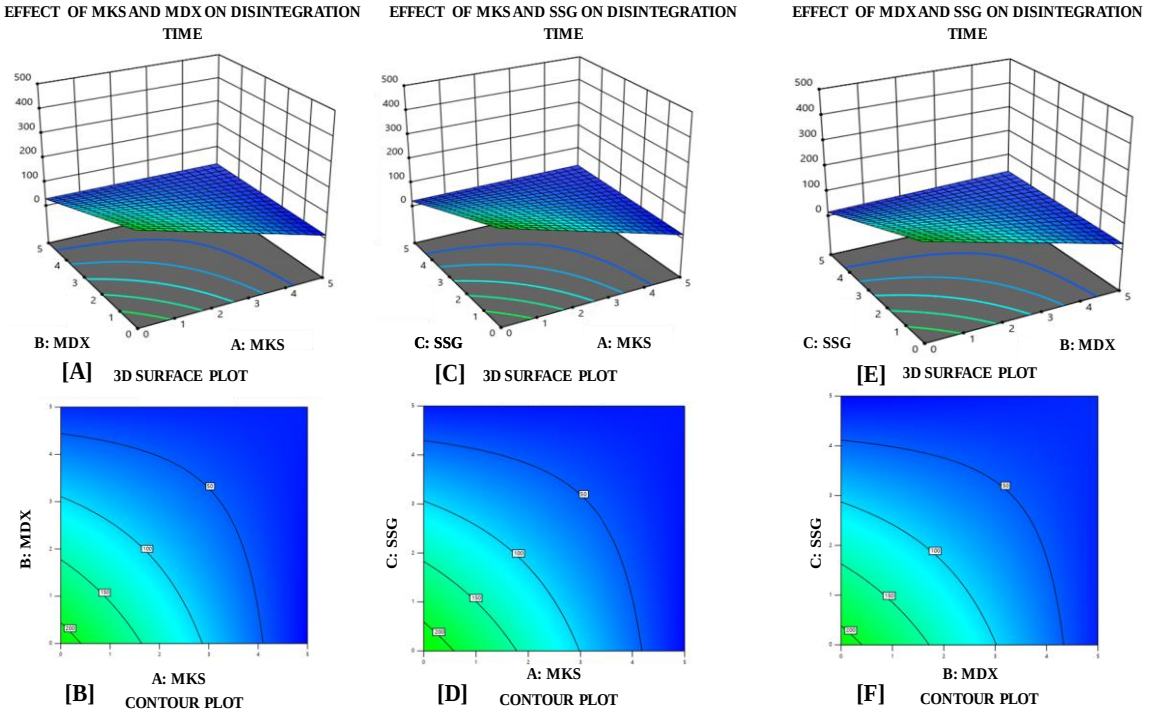

Fig. 3: Images of 3D surface response plots and contour plots displaying the effect of the combination of super disintegrants on *in vitro* disintegration time

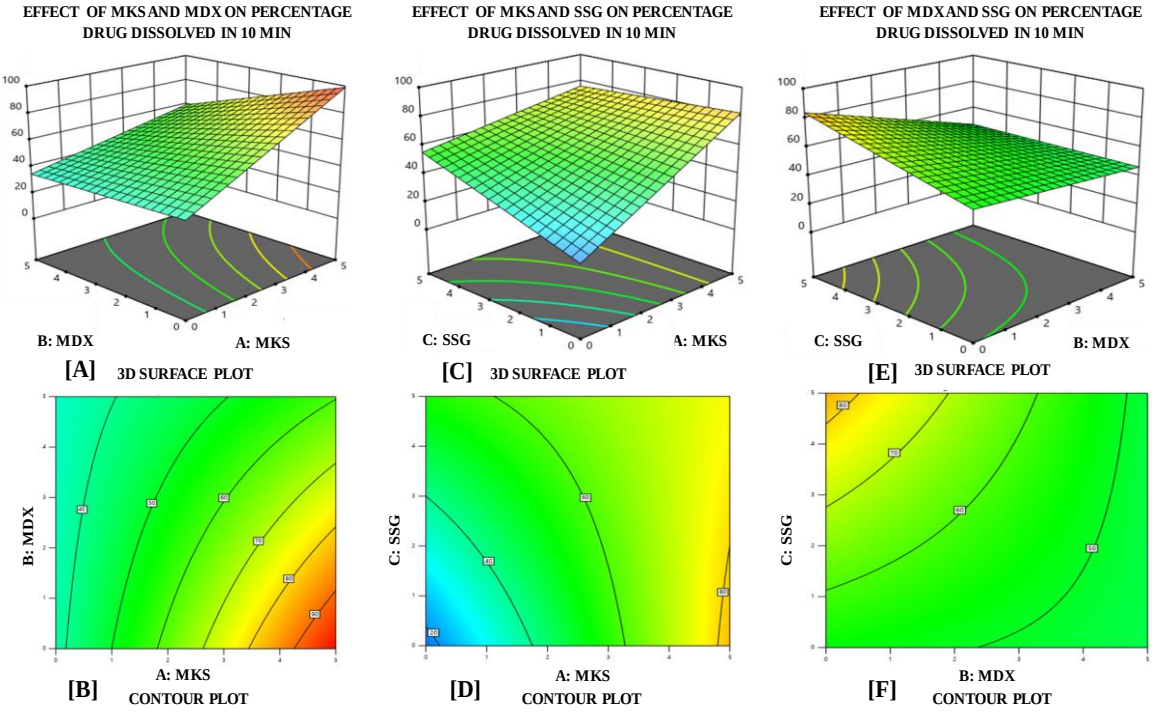

Fig. 4: Images of 3D response surface plots and contour plots displaying the effect of the combination of super disintegrants on the percentage of drug dissolved in 10 min

Saturated solubility of RZN under different temperatures

The saturated solubility of RZN increases with temperature, being relatively low at room temperature (25 °C), higher at body temperature (37 °C), and significantly higher at elevated temperatures (50 °C and above).

Characterization of RZN FDFs

No morphological changes were observed in the RZN FDFs across all formulations. The films remained transparent and exhibited a smooth texture. The choice of HPMC as the polymer was made because it could produce a transparent, smooth texture. The prepared RZN FDFs were found to weigh between 97.54±0.72 mg to 99.88±0.50 mg, as shown in fig. 5A. This consistency suggests that the film preparation process was well-controlled and demonstrates a high level of uniformity. The films exhibited a thickness ranging from 0.212±0.02 mm and 0.364±0.07 mm, as shown in fig. 5B. Thickness and weights of different films increased with the polymer concentration [38].

The film disintegration time ranged from 13.45±1.05 to 418.14±1.06 sec, with the formulation RF2 prepared with 5% MKS showed the least disintegration time of 13.45±1.05 sec, as shown in table 6. Oral films typically have disintegration times ranging from 5 to 30 sec, although this can vary based on the formulation's ingredients. One study suggested that a good disintegration time for an oral film is within 1 min. In examining different formulas, it was observed that the formulations with higher extract content exhibited longer disintegration times, likely due to increased film thickness. Previous research supports this, indicating that thicker films generally require more time to disintegrate. In this study, disintegration times ranged from 13.45±1.05 to 418.14±1.06 sec, with the RF2 formulation (containing 5% MKS) showing the shortest disintegration time of 13.45±1.05 sec (table 6) [39].

The film's surface pH measurements ranged between 6.21±0.64 and 6.92±0.66 as shown in fig. 5G, indicating that the film pH closely matches the pH of saliva. The results were close to the neutral pH for all the batches, suggesting that the films are non-irritating in the oral cavity.

The tensile strength of the films ranged from 1.85±0.55 MPa to 3.92±0.67 MPa as shown in fig. 5C. The increase in the polymer concentration significantly enhanced the tensile strength due to the creation of a densely packed matrix and a robust polymer chain network. These results align with findings by Reddy TUK *et al.* [40], who discovered that a considerable increase in polymer concentration affected tensile strength. The percentage elongation of the films was found to be between 13.64±0.93% to 25.34±0.25% as shown in fig. 5E. Incorporating a 5% disintegrating agent into the films significantly impacts their mechanical properties, particularly the percentage elongation. The increase in percentage elongation can be attributed to the replacement of intermolecular bonds in the polymer matrix with a plasticizer. These findings are consistent with those reported by Shah KA *et al.*, who identified PG as the best plasticizer [41].

The folding endurance of the films was ranged from 105.00±0.63 to 135.00±0.49, as shown in fig. 5F. Higher folding endurance indicates greater mechanical strength of the films. Furthermore, when the plasticizer is present in the right amounts, the film remains flexible and doesn't break easily even after repeated folding. These findings are consistent with those of Smith *et al.*, who discussed the impact of plasticizer and polymer concentration [42].

The percentage of moisture loss in the films ranged from 1.02±0.70% to 1.8±0.45%w/w, as shown in fig. 5G. The percentage moisture uptake ranged from 2.13±0.74% to 2.98±0.71% w/w as given in fig. 5G. The films' ability to absorb moisture is crucial, as it affects their mechanical characteristics. An overall pattern was observed, with rising plasticizer and polymer levels leading to increased moisture uptake.

Table 6: Evaluation parameters (Disintegration time in sec, percentage dissolved in 10 min) of RZNFDFs

Formulations	Disintegration time in sec	Percentage dissolved in 10 min
RF1	418.14±1.06	8.14±0.58
RF2	13.45±1.05	99.28±0.96
RF3	30.36±1.12	84.54±0.60
RF4	19.20±1.02	90.24±0.17
RF5	15.32±2.02	94.12±0.47
RF6	14.40±1.19	98.98±0.81
RF7	28.31±2.12	87.23±0.70
RF8	31.30±0.50	71.24±0.07

Data are expressed as mean ±SD, n=3

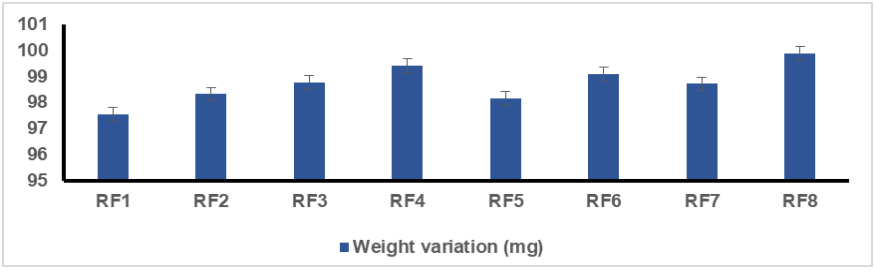

A

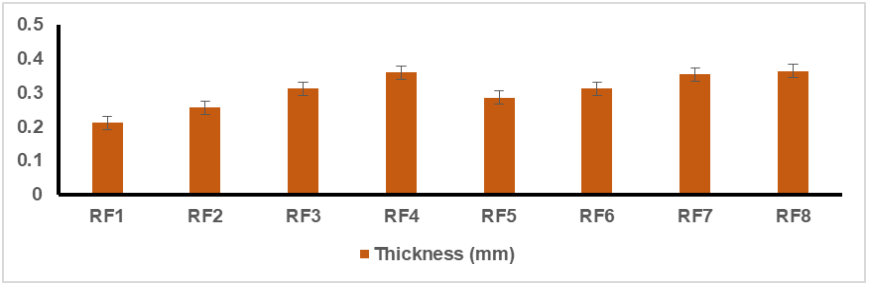

B

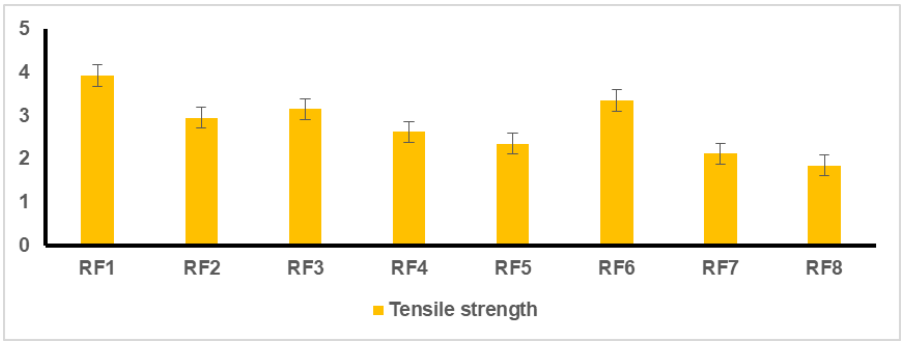

C

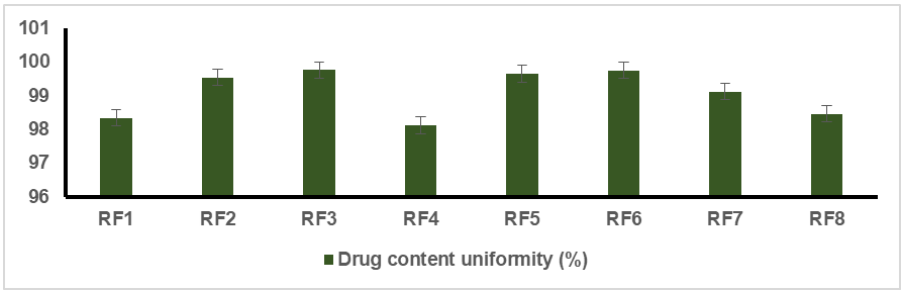

D

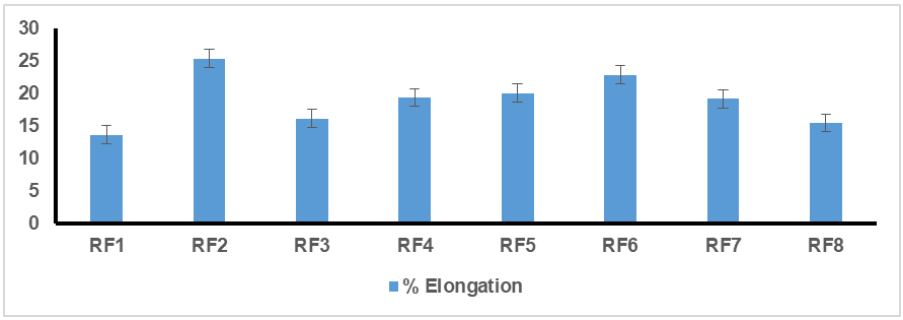

E

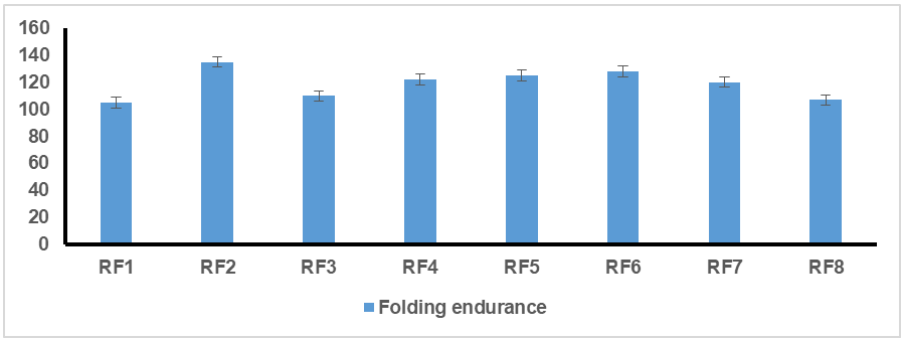

F

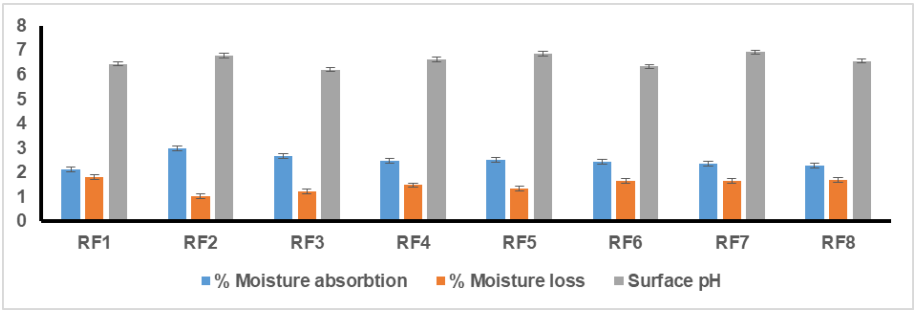

G

Fig. **5: Graphical presentation of weight variation (A), Thickness (B), Tensile strength(C), Drug content uniformity (D), Percentage elongation (E), Folding endurance (F), Percentage moisture uptake, percentage moisture loss and surface pH (G) of all batches (RF1–RF8)-Data in the fig. are expressed as mean ±SD, n=3**

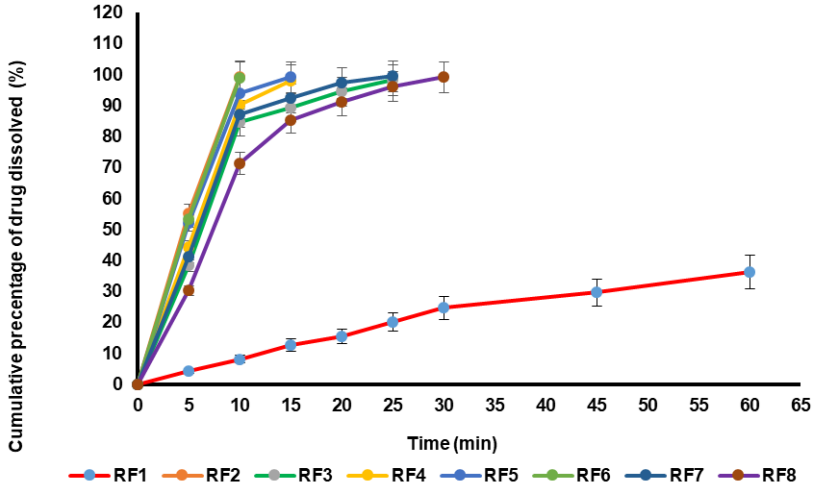

Fig. 6: Cumulative percentage of drug dissolved from the formulation RF1 to RF8, data in the fig. **are expressed as mean ±SD, n=3**

Pharmacokinetic data analysis

For pharmacokinetic studies in rats, the plasma concentration versus time profile is shown in fig. 7. Pharmacokinetic parameters including T_{max}, C_{max}, AUC, bioavailability (BA), rate of elimination constant (K_e), and rate of absorption constant (K_a) were calculated from the plasma profile using MS Excel. The RZN plasma concentration after the oral administration in pure form (A) and in fast-dissolving film form (B) is depicted. From the plot, it can be concluded that after the administration of RZN FDFs the plasma concentration is higher initially within a short period and reaches its C_{max} concentration. This indicates that the FDFs formulation allow for maximum drug absorption within 1-2 h.

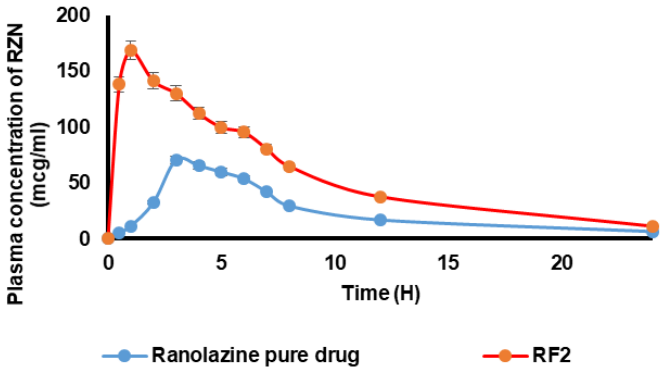

Fig. 7: Plasma concentration of RZN pure drug and formulation RF2-data in the fig. are expressed as mean ±SD, n=3

Table 7: Summary of pharmacokinetic parameters of RZN pure drug and optimized RZN fast-dissolving film RF2 employing MKS

Pharmacokinetic parameter	Pure RZN (A)	Optimized formulation (RF2)
C_{max} (µg/ml)	70.1	168.92
T_{max}(h)	3.00	1.00
$AUC_{0-\infty}$ (mcg. h/ml)	648.73	1488.86
BA(%)	-	229.50
$K_a(h^{-1})$	0.049	0.059
$K_{el}(h^{-1})$	0.112	0.101

Table 8: Summary of stability studies

Retest time for optimized formulation	FE (sec)	DT (Sec)	Percent dissolved in 10 min (%)	Drug content (%)
Before stability (RF2)	135.33±0.58	13.01±1.02	99.78±0.92	99.54±0.78
After stability (RF2)	136.33±1.53	12.30 ±0.30	99.54±0.36	99.26 ±0.26

Data are expressed as mean ±SD, n=3

CONCLUSION

This study developed and evaluated the FDFs of antihypertensive drug RZN using a 2^3 factorial design with super disintegrants MKS, MDX and SSG. The films were prepared by solvent casting technique and were assessed for the key parameters like disintegration time and drug dissolution. Formulation RF2, with 5% MKS, showed the shorter disintegration time and highest drug dissolution, making it

the optimized formulation. This research introduced MKS as a novel and superior super disintegrant, significantly improving drug delivery compared to traditional options. Statistical analysis confirmed MKSs positive impact, through interactions between the disintegrants were generally less favourable. The study suggests that MKS could enhance drug delivery, prompt sustainability, and reduced costs, allowing for future research into its industrial sustainability and pharmacokinetic advantages in various pharmaceutical formulations.

FUNDING

Nil

AUTHORS CONTRIBUTIONS

Gayatri Devi Medisetty-method selection, compilation of data and writing the original draft. Santosh Kumar Rada-Review, compilation of data, editing and supervision**.**

CONFLICT OF INTERESTS

Declared none

REFERENCES

1. Yir Erong B, Bayor MT, Ayensu I, Gbedema SY, Boateng JS. Oral thin films as a remedy for noncompliance in pediatric and geriatric patients. Ther Deliv. 2019 Jul;10(7):443-64. doi: 10.4155/tde-2019-0032, PMID 31264527.
2. Dixit RP, Puthli SP. Oral strip technology: overview and future potential. J Control Release. 2009 Oct;139(2):94-107. doi: 10.1016/j.jconrel.2009.06.014, PMID 19559740.
3. Darshan PR, Preethi S. Fast dissolving films an innovative approach for delivering nutraceuticals. In: Patel PB, editor. Innovative approaches in oral drug delivery. Elsevier; 2023. p. 361-96.
4. Lee Y, Kim K, Kim M, Choi DH, Jeong SH. Orally disintegrating films focusing on formulation manufacturing process and characterization. J Pharm Investig. 2017 Feb 27;47(3):183-201. doi: 10.1007/s40005-017-0311-2.
5. Bhyan B, Jangra S, Kaur M, Singh H. Fast dissolving films: innovations in formulation and technology. Int J Pharm Sci Rev Res. 2011 Jul;9(2):50-5.
6. Qin ZY, Jia XW, Liu Q, Kong BH, Wang H. Fast dissolving oral films for drug delivery prepared from chitosan/pullulan electrospinning nanofibers. Int J Biol Macromol. 2019 Sep 15;137:224-31. doi: 10.1016/j.ijbiomac.2019.06.224, PMID 31260763.
7. Liew KB, Odeniyi MA, Peh KK. Application of freeze drying technology in manufacturing orally disintegrating films. Pharm Dev Technol. 2016;21(3):346-53. doi: 10.3109/10837450.2014.1003657, PMID 25597618.
8. Cilurzo F, Cupone IE, Minghetti P, Buratti S, Selmin F, Gennari CG. Nicotine fast dissolving films made of maltodextrins: a feasibility study. AAPS Pharm Sci Tech. 2010;11(4):1511-7. doi: 10.1208/s12249-010-9525-6, PMID 20936440.
9. Drago E, Campardelli R, Lagazzo A, Firpo G, Perego P. Improvement of natural polymeric films properties by blend formulation for sustainable active food packaging. Polymers (Basel). 2023;15(9):1511. doi: 10.3390/polym15092231, PMID 37177377.
10. Darekar A, Sonawane M, Saudagar R. Formulation and evaluation of orally fast dissolving wafer by using natural gum: review article. Int J Curr Pharm Rev Res. 2017 Jun;8(3):1-7. doi: 10.25258/ijcprr.v8i03.9214.
11. Lebaka VR, Wee YJ, YE W, Korivi M. Nutritional composition and bioactive compounds in three different parts of mango fruit. Int J Environ Res Public Health. 2021 Jan 16;18(2):741. doi: 10.3390/ijerph18020741, PMID 33467139.
12. Punia Bangar S, Kumar M, Whiteside WS. Mango seed starch: a sustainable and eco friendly alternative to increasing industrial requirements. Int J Biol Macromol. 2021 Jul 31;183:1807-17. doi: 10.1016/j.ijbiomac.2021.05.157, PMID 34051254.
13. Kusuma A, Santosh Kumar R. Optimization of fast dissolving tablets of carvedilol using 2^3 factorial design. Int J App Pharm. 2024 Jan;16(1):98-107. doi: 10.22159/ijap.2024v16i1.49535.
14. Rani N, Dev D, Prasad DN. Recent trends in developments of super disintegrants: an overview. J Drug Delivery Ther. 2022 Jan;12(1):163-9. doi: 10.22270/jddt.v12i1.5148.
15. Shahrim NA, Sarifuddin N, Ismail H. Extraction and characterization of starch from mango seeds. J Phys: Conf Ser. 2018;1082:012019. doi: 10.1088/1742-6596/1082/1/012019.
16. Noor F. Physicochemical properties of flour and extraction of starch from jackfruit seed. Int J Nutr Food Sci. 2014 Aug;3(4):347-54. doi: 10.11648/j.ijnfs.20140304.27.
17. Sonthalia M, Sikdar S. Production of starch from mango (Mangifera indica L.) seed kernel and its characterization. Int J Tech Res Appl. 2015 May-Jun;3(3):346-9.
18. Patil PD, Gokhale MV, Chavan NS. Mango starch: its use and future prospects. Innov J Food Sci. 2014 Oct;2(1):29-30.
19. Hassan LG, Muhammad A, Aliyu R, Idris Z, Izuagie T, Umar K. Extraction and characterisation of starches from four varieties of Mangifera indica seeds. IOSR-JAC. 2013 Feb;3(6):16-23. doi: 10.9790/5736-0361623.
20. Omoregie Egharevba H. Chemical properties of starch and its application in the food industry. Chem Prop Starch. 2019. doi: 10.5772/intechopen.87777.
21. Ratnayake WS, Wassinger AB, Jackson DS. Extraction and characterization of starch from alkaline cooked corn masa. Cereal Chem. 2007 Jul;84(4):415-22. doi: 10.1094/CCHEM-84-4-0415.
22. Vemuri VV, Nalla S, Gollu G, Mathala N. Cramming on potato starch as a novel superdisintegrant for depiction and characterization of candesartan cilexetil fast dissolving tablet. Int J Biol Macromol. 2021 Feb;45(2):137-47.
23. Jasvanth E, Teja D, Mounika B, Nalluri BN. Formulation and evaluation of ramipril mouth dissolving films. Int J Appl Pharm. 2019;11(3):124-9.
24. Jassim ZE, Mohammed MF, Sadeq ZA. Formulation and evaluation of fast-dissolving film of lornoxicam. Asian J Pharm Clin Res. 2018 Sep;11(9):217-23. doi: 10.22159/ajpcr.2018.v11i9.27098.
25. Kawale KA, Autade NB, Narhare HS, Mhetrea RL. A review on fast dissolving oral film. Asian J Pharm Clin Res. 2023 Oct;16(10):7-17. doi: 10.22159/ajpcr.2023.v16i10.48099.
26. Ponnaganti H, Sakeena F. Formulation and evaluation of oral fast dissolving films of naproxen sodium. Int J Curr Pharm Res. 2022 Mar;14(2):48-53.
27. Sarfaraz MD, Kumar S, Doddayya H. Fabrication and evaluation of mouth-dissolving films of domperidone. Int J Curr Pharm Res. 2023 Jan;15(2):36-43.
28. Farooqui P, Gude R. Formulation development and optimisation of fast dissolving buccal films loaded glimepiride solid dispersion with enhanced dissolution profile using central composite design. Int J Pharm Pharm Sci. 2023 Jun;15(6):35-54. doi: 10.22159/ijpps.2023v15i6.47992.
29. RKD, Keerthy HS, Yadav RP. A review on fast dissolving oral films. Asian J Pharm Res Dev. 2021 Jun;9(3):122-8. doi: 10.22270/ajprd.v9i3.969.
30. Birla N, Mandloi K, Mandloi R, Pillai S. Formulation and evaluation of quick dissolving films of promethazine hydrochloride. Res J Pharm Technol. 2017;10(4):1025-8. doi: 10.5958/0974-360X.2017.00185.8.
31. Deepthi PR, Kumar KS. Formulation and evaluation of amlodipine besylate oral thin films. Int J Pharm Sci Res. 2016 Jan;7(1):199-205.
32. Torgal T, Borkar S, Bhide P, Arondekar A. Formulation development and evaluation of fast dissolving films of ebastine. Int J Curr Pharm Sci. 2020 Sep;12(5):111-5. doi: 10.22159/ijcpr.2020v12i5.39782.
33. Sevinç Özakar R, Ozakar E. Current overview of oral thin films. Turk J Pharm Sci. 2021 Feb 25;18(1):111-21. doi: 10.4274/tjps.galenos.2020.76390, PMID 33634686.
34. Roy A, Arees R. Blr M. Formulation development of oral fast dissolving films of Rupatadine fumarate. Asian J Pharm Clin Res. 2020 Nov;13:67-72.
35. Sultana F, Arafat Y, Pathan SI. Preparation and evaluation of fast-dissolving oral thin film of caffeine. Int J Pharm Biol Sci. 2013 Jan;3:153-61.
36. Rai JP, Mohanty PK, Prajapati M, Sharma VK. *In vivo* bioavailability study of telmisartan complex in wistar rats. J Adv Sci Res. 2020 Jan;11(4)Suppl 9:146-9.

37. Patel JM, Dhingani AP, Garala KC, Raval MK, Sheth NR. Development and validation of bioanalytical HPLC method for estimation of telmisartan in rat plasma: application to pharmacokinetic studies. Dhaka Univ J Pharm Sci. 2012 Dec;11(2):121-7. doi: 10.3329/dujps.v11i2.14562.
38. Nurhabibah N, Sriarumtias FF, Fauziah S, Auliasari N, Hindun S. Formulation and evaluation fast disintegrating film salbutamol sulfat using HPMC E15. J Phys: Conf Ser. 2019;1402(5):1-8. doi: 10.1088/1742-6596/1402/5/055093.
39. Zubaydah WO, Sahumena MH. Fast-dissolving oral film salbutamol sulphate using HPMC polymer. Indones J Chemom Pharm Anal. 2021;3:133-42.
40. Reddy TU, Reddy KS, Manogna K, Thyagaraju K. A detailed review on fast dissolving oral films. J Pharm Res. 2018;8(6):1351-62.
41. Shah KA, Gao B, Kamal R, Razzaq A, QI S, Zhu QN. Development and characterizations of pullulan and maltodextrin-based oral fast-dissolving films employing a box-Behnken experimental design. Materials (Basel). 2022 May 18;15(10):3591. doi: 10.3390/ma15103591, PMID 35629620.
42. Smith A, Srinivasan V, Wallace L. Influence of plasticizer and polymer concentration on the mechanical properties of pharmaceutical films. J Pharm Sci. 2019;108(5):1672-83.